



Structural Origins of the Anisotropic Thermal Expansion of BINOL Crystals

Paul G. Waddell¹

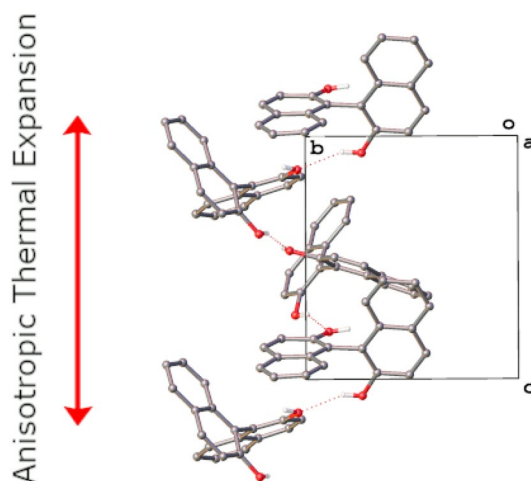
Received: 16 February 2024 / Accepted: 14 March 2024
© The Author(s) 2024

Abstract

Measurement of the unit cell of (R)-BINOL over a 200° temperature range (300–100 K) reveals an anisotropic contraction where the c-axis contracts *ca.* 2.3% compared to a *ca.* 0.45% contraction of the a and b axes, a *ca.* six-fold difference in linear thermal expansion coefficient. This contraction corresponds to a decrease in the helical pitch of the 3₁ screw axis in the [001] direction. The anisotropic nature of the contraction is rationalised by a thorough analysis of intermolecular contacts within the crystal and their impact on the conformation of the molecule and crystal packing.

Graphical Abstract

The crystal structure of (R)-BINOL exhibits a pronounced anisotropic thermal expansion.



Keywords BINOL · Variable temperature · Supramolecular spring · Anisotropic thermal expansion

Introduction

As a general rule, materials expand with increasing temperature as the amplitudes of atomic vibrations are increased. Typically, this effect is noticeable yet modest and the

contraction/expansion observed as a result of the changing temperature is approximately equal in each direction [1]. In certain cases however, changes in temperature can induce more pronounced conformational changes that allow for a greater degree of expansion in one or more specific directions. This phenomenon is known as anisotropic thermal expansion.

Such anisotropic expansion is exemplified by the ability of structures that exhibit helical motifs to act as ‘supramolecular springs’ [2, 3]. In such materials, changes to the

✉ Paul G. Waddell
paul.waddell@ncl.ac.uk

¹ Faculty of Science Agriculture and Engineering,
Newcastle University, Bedson Building,
Newcastle upon Tyne NE1 7RU, UK

helical pitch can be induced by changes in pressure and/or temperature [4]. The spring-like quality arises as a direct result of the anisotropic nature of the response to the forces acting upon the material.

The study of thermoresponsive materials such as these has seen an increase in interest of late and such thermomechanical substances have potential in a wide range of applications [5, 6]. As materials in which mechanical responses can be induced at a molecular level, the study of molecular or supramolecular spring systems will help drive the development of molecular machines [7].

This development will rely on examining the relationship between the structures of these materials and their properties. Through an understanding of the interplay between the various solid-state interactions that influence the packing in those crystal structures observed to exhibit unusual behaviours under certain stimuli, it should be possible to use this knowledge to develop materials with bespoke properties tailored to specific applications [8].

(*R*)-(+)–1,1'-Bi(2-naphthol) ((*R*)-BINOL) is a simple organic molecule that forms hydrogen-bonded supramolecular helices in the solid-state (Fig. 1) [8]. Despite various iterations of the crystal structure of (*R*)-BINOL being published over the years [9–12], the first structure measured at cryogenic temperature was only recently reported [13]. In this low temperature structure the *c*-axis was reported to be *ca.* 0.2 Å shorter than that measured for any of the structures at room temperature. This contraction is nearly

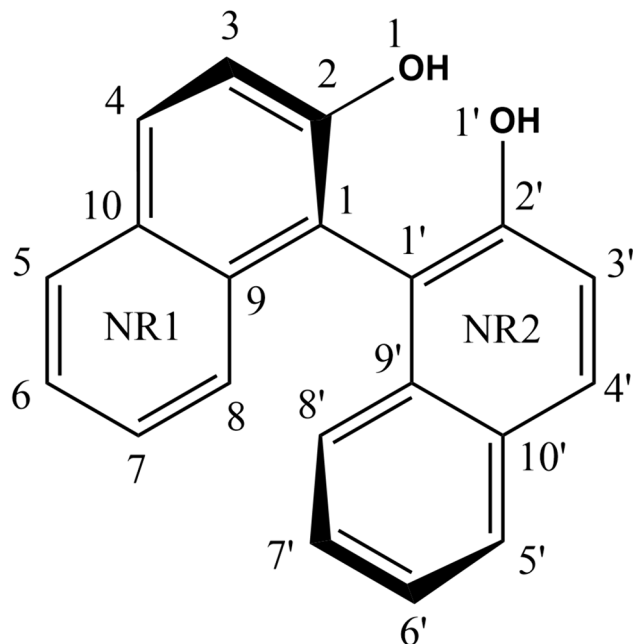


Fig. 1 (*R*)-BINOL with atomic numbering scheme and naphthalene rings (NR) labelled

10-times greater than that observed for the other two axes, a classic example of anisotropic thermal expansion.

The chiral nature of (*R*)-BINOL (an instance of axial chirality), its helical solid-state structure and its highly directional conformational flexibility makes it ideal for incorporation into more complex molecules that may exhibit spring-like compressibility (Fig. 2) [14]. Due to its simplicity, studying the compound in isolation and without additional structural variables should provide some fundamental insights into how similar biaryl systems behave and the potential effects of including them in such systems.

This work comprises an in-depth, variable-temperature analysis of the crystal structure of (*R*)-BINOL highlighting the anisotropic thermal expansion observed and demonstrates that this is a consequence of a very subtle change in molecular conformation.

Experimental

(*R*)-BINOL was purchased from Sigma-Aldrich and used without any further purification. Crystals suitable for single crystal X-ray diffraction analysis were grown via slow evaporation from a solution of the compound in toluene.

Single crystal diffraction data were collected on an Xcalibur, Atlas, Gemini ultra diffractometer using copper radiation ($\lambda_{\text{CuK}\alpha} = 1.54184 \text{ \AA}$) and the temperature of the sample was controlled using an Oxford Cryosystems CryostreamPlus open-flow N_2 cooling device. The temperature was lowered from 300 to 100 K in 10 K steps at a rate of 180 K/h. Five datasets were collected at 50 K intervals between 300 and 100 K and unit cell dimensions were measured at 10 K steps across the same range. All datasets and unit cell parameters were collected and measured respectively using the same crystal on the same mount without removing it from the goniometer.

Intensities were corrected for absorption empirically using spherical harmonics. Cell refinement, data collection and data reduction were undertaken via the software CrysAlisPro [15].

All structures were solved using XT [16] and refined by XL [17] using the Olex2 interface [18] (Fig. 3). All

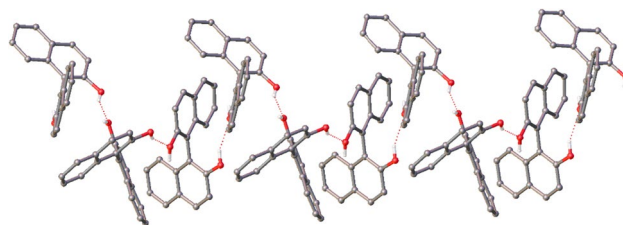


Fig. 2 The helical hydrogen bonded chain in the [001] direction in the structure of (*R*)-BINOL

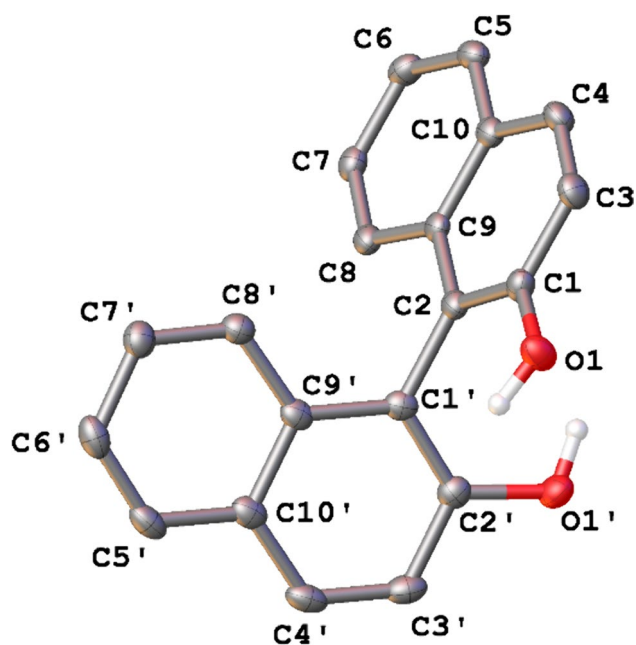


Fig. 3 The asymmetric unit of the structure of (R)-BINOL at 100 K with ellipsoids drawn at the 50% probability level. Hydrogen atoms, with the exception of those bound to oxygen, have been omitted for clarity

non-hydrogen atoms were refined anisotropically and hydrogen atoms were positioned with idealised geometry, with the exception of those bound to oxygen, the positions of which were located using peaks in the Fourier difference map. The displacement parameters of the hydrogen atoms were constrained using a riding model with $U_{(H)}$ set to be an appropriate multiple of the U_{eq} value of the parent atom.

The thermal expansion coefficients were calculated using the web-based tool, PASCAL [19].

Results and Discussion

The anisotropic nature of the contraction/expansion of crystals of BINOL is attested to by the variation in the unit cell parameters of the crystal structure over the 300–100 K temperature range. Both the *a* and *b* axes, which are constrained to be equivalent for a trigonal crystal system, and the *c*-axis are observed to vary linearly with temperature. However, where *a* and *b* decrease by *ca.* 0.05 Å with a linear thermal expansion coefficient of $\alpha_L(a, b) = 18.1 \times 10^{-6} \text{ K}^{-1}$ at 100 K, *c* decreases by *ca.* 0.25 Å with $\alpha_L(c) = 112.2 \times 10^{-6} \text{ K}^{-1}$, almost six times what might be considered the norm [1]. Over this range the *c*-axis also goes from being the longest to the shortest axis with all three axes being approximately equivalent at around 240 K (Fig. 4).

As the helical motif completes a full turn along the length of the *c*-axis, the contraction of *c* corresponds directly to a

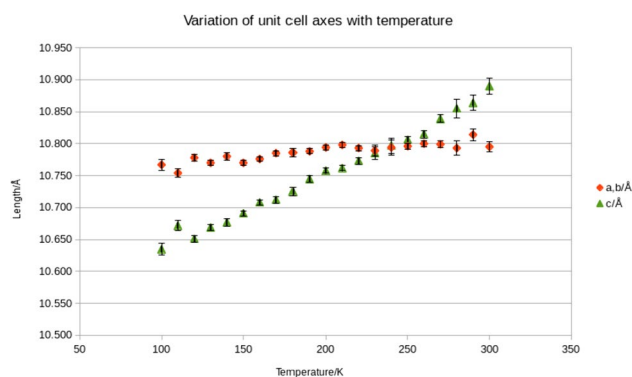


Fig. 4 The variation in the lengths of the unit cell axes of (R)-BINOL with temperature from 100 to 300 K

shortening of the helical pitch of the 3_1 screw axis. The helix in this case is formed of a C(7) hydrogen bonding motif [20]. Given this, and that the *c*-axis is the only direction in which classical hydrogen bonds propagate, it might be reasonable to suspect that the pronounced contraction along this axis can be attributed to a shortening of these hydrogen bonding interactions bringing the molecules closer together in this direction. Superficially, this could indeed be the case; the distance between hydrogen bond donor and acceptor decreases from 2.963(3) Å at 300 K to 2.914(2) Å at 100 K (Table 1). However, by measuring the angle of the hydrogen bond vector to the *c*-axis it is possible to calculate the contribution of the hydrogen bond to the *c*-axis. Interestingly, as the general trend in this angle sees it become smaller at lower temperature, this contribution to *c* actually increases as the temperature is reduced, from 0.717(2) Å at 300 K to 0.735(2) Å at 100 K. This change may be subtle but it indicates that the structural origins of the anisotropy of the contraction are more complicated.

As the lengths of the hydrogen bonds do not fully explain the contraction along the *c*-axis, and indeed provide a somewhat counter-intuitive expansion in terms of their contribution to *c*, analysis of the conformation may shed some light on the mechanism of the contraction. A molecule of BINOL exhibits a certain degree of rotational freedom about the C1–C1' bond and therefore there can be some variation in the angle between the two naphthyl groups. Depending

Table 1 Hydrogen bond geometry for (R)-BINOL from 100 to 300 K

(K)	O1–H1/Å	H1···O1 ¹ /Å	O1···O1 ¹ /Å	O1–H1···O1 ¹ /°
100	0.84(3)	2.13(3)	2.914(2)	154(3)
150	0.84(3)	2.17(3)	2.923(2)	149(3)
200	0.88(3)	2.15(3)	2.935(2)	148(3)
250	0.85(4)	2.18(4)	2.949(2)	150(3)
300	0.87(4)	2.20(4)	2.963(2)	146(4)

on the orientation of the molecule relative to the *c*-axis, an increase in the angle could correspond to an expansion or contraction of this axis. In this case the molecules are orientated in such a way that a decrease in this interplanar angle will result in a reduction of the helical pitch of the hydrogen bonding motif as this reduced angle will bring O1 and O1' on the same molecule closer together, resulting in a decrease in the length of *c*.

A general trend of decreasing torsion angle (C2–C1–C1'–C2') in the structure of BINOL is observed; upon cooling from 300 to 100 K, this angle decreases by *ca.* 2° (Fig. 5). The overall result of this subtle change in torsion angle about C1–C1' is that the entire hydrogen-bonded chain of molecules contracts in a manner reminiscent of a pantograph or scissors mechanism. It is this change in the conformation of the molecule that accounts for the relatively drastic contraction of *c* relative to that of *a* and *b*. Conversely, it is the rigidity of the BINOL molecule in the directions orientated along *a* and *b* that accounts for the lesser degree of contraction in these directions.

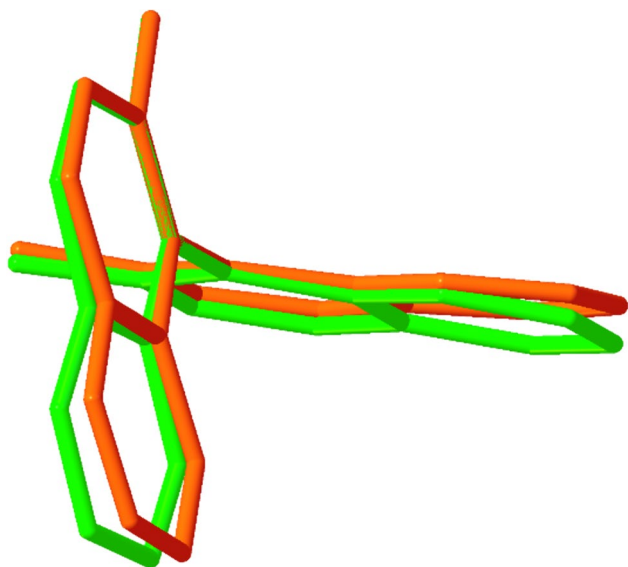


Fig. 5 An overlay of the structure of (R)-BINOL at 100 K (green) and 300 K (orange)

It is clear from this analysis that the shortening of the hydrogen bonds and coincident conformational perturbation of the BINOL molecule is the root cause of the anisotropic contraction in these crystals. However, more subtle conformational changes are also evident in the structure which can be attributed to less obvious intermolecular interactions whose impact on the conformation becomes more pronounced at lower temperature. This can be observed in the analysis of the geometry of the naphthyl groups.

Though ideally planar, the naphthyl groups of BINOL exhibit slight deviations from planarity which can be described in terms of the 'twist' and 'fold' angles between the two six-membered rings that comprise the naphthyl moiety. In this analysis the two naphthyl groups are referred to as NR1, which comprises atoms C1–C10, and NR2, comprising atoms C1'–C10' (Table 2).

As the temperature decreases, a reduction in the fold angle for both NR1 and NR2 is observed corresponding to a flattening out of the naphthyl groups. This is consistent with the change in the C2–C1–C1'–C2' torsion angle, which also represents a move towards a more planar conformation. The twist angle of NR1 further reflects this general trend as it too decreases very slightly (*ca.* 0.3°) over the temperature range studied. Overall, the root mean squared deviation (RMSD) of NR1 decreases from 0.016 Å at 300 K to 0.012 Å at 100 K.

Bucking this trend towards greater planarity is the twist angle of NR2, which increases by nearly 0.5° resulting in an overall increase in the RMSD of NR2. This increased twisting and the lack of a similar effect in NR1 can be rationalised by considering the close contacts involving the atoms of the naphthyl groups.

Close contacts other than hydrogen bonds were identified by using CrystalExplorer to calculate Hirshfeld surfaces for the molecule at each temperature [21]. By mapping the property D_{norm} onto the surface, contacts that are closer than van der Waals interactions appear as red spots (Fig. 6). Four such contacts were observed for BINOL, two of which correspond to contacts between atoms of NR1 and those of NR1 on an adjacent molecule with the remaining two being between carbon atoms on NR1 and hydrogen atoms of NR2 on an adjacent molecule (Table 3). As these contacts are all of the type C–H...D (where D is a carbon atom, heteroatom

Table 2 Selected geometric parameters for (R)-BINOL from 100–300K

(K)	C1–C2–C1'–C2'°	Twist°(NR1)	Twist°(NR2)	Fold°(NR1)	Fold°(NR2)	RMSD/Å (NR1)	RMSD/Å (NR2)
100	– 76.5(3)	0.68(1)	2.06(1)	1.53(1)	1.91(1)	0.016	0.028
150	– 76.0(3)	0.57(1)	2.22(1)	1.44(1)	1.70(1)	0.015	0.028
200	– 75.4(3)	0.51(1)	2.35(1)	1.30(1)	1.63(1)	0.014	0.029
250	– 74.9(3)	0.44(1)	2.44(1)	1.18(1)	1.62(1)	0.013	0.030
300	– 74.5(3)	0.41(1)	2.49(1)	1.08(1)	1.58(1)	0.012	0.030

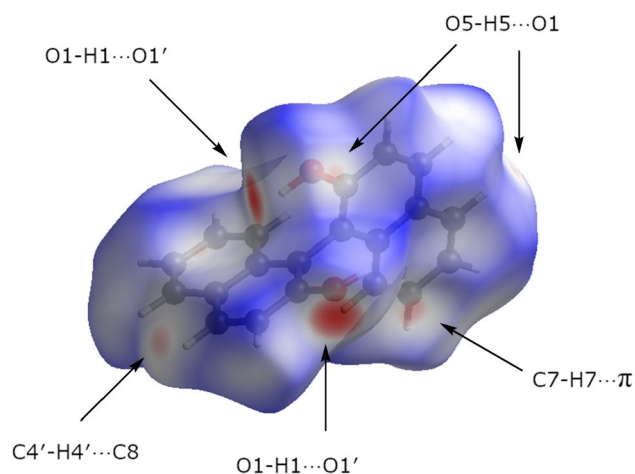


Fig. 6 Hirshfeld surface calculated for a molecule of the crystal structure of (R)-BINOL at 100 K

Table 3 Selected inter-molecular distances for (R)-BINOL from 100 to 300 K

(K)	O1...H5/Å	H7...π/Å	C7...H8'/Å	C8...H4'/Å
100	2.65(1)	2.74(1)	2.77(1)	2.68(1)
150	2.67(1)	2.77(1)	2.79(1)	2.70(1)
200	2.69(1)	2.79(1)	2.82(1)	2.71(1)
250	2.71(1)	2.82(1)	2.85(1)	2.73(1)
300	2.74(1)	2.86(1)	2.87(1)	2.75(1)

or π -system) they can be characterised as weak hydrogen bonds [22]. Each of these interactions contracts by *ca.* 0.1 Å on average upon cooling from 300 to 100 K.

The shortest and most likely strongest of these interactions is a C–H...O type interaction observed between H5 and O1. The interatomic distance contracts from 2.74(1) to 2.65(1) Å over the temperature range studied. The second interaction involving two adjacent N1 moieties is an edge-to-face interaction between the two naphthyl groups. Here, H7 appears to point directly into the centre of the C5–C10 aromatic ring to form a C–H... π interaction with an H...ring centroid distance ranging from 2.86(1) to 2.74(1) Å over the temperature range studied.

Considering the packing about NR1, these two interactions appear to work in tandem to pull opposite ends of this naphthyl group in opposite directions as they are close in angle to the normal of the NR1 plane. This could very well facilitate and stabilise the decrease in the C2–C1–C1'–C2' torsion angle observed upon cooling, which is key to the reduction of the helical pitch of the hydrogen bonding motif.

There are also two close contacts relating to weak hydrogen bonding interactions involving NR2. For both of

these it is hydrogen atoms on NR2 that act as the donors. One is between H4' and C8 and appears to be directly competing with the C–H... π involving H7. Though in this case the closest contact is shorter than that for the C7–H7... π interaction at all temperatures, C8...H4' is most likely weaker in nature as the C–H...D angle is more acute, the drop-off in hydrogen bond strength being more pronounced with a smaller angle than with a larger distance [23], and the distance from H4' to the ring centroid greater (2.93(1) Å at 100 K). The C7–H7... π interaction is therefore able to out-compete C8...H4' and affect the reduction in the C2–C1–C1'–C2' torsion angle.

The other interaction involving NR2 is between H8' and C7. It is similar in nature to the C8...H4' interaction. Together these two interactions act in opposite directions and, as the angle of the interaction vector is closer to the plane of the naphthyl group than the plane normal, are most likely the root of the twist observed in this moiety.

Conclusions

Measuring the unit cell parameters of a crystal of (R)-BINOL and calculating the thermal expansion coefficient revealed that they exhibit a significant anisotropic thermal expansion. Analysis of the molecular geometry gleaned from structure determinations of (R)-BINOL at various temperatures revealed that subtle changes in the torsion angle between the naphthalene rings and changes in the twisting and folding of the fused rings contribute more to the expansion/contraction than changes in the hydrogen bond distances. The weak interactions that appear to influence these geometric changes were identified and rationalised with closer C–H... π distances at lower temperatures influencing the conformation of the fused rings and overall molecular conformation.

These observations should prove useful in terms of crystal engineering as they will inform the development of molecular systems incorporating BINOL allowing this anisotropic thermal expansion property to be exploited in spring-like molecular machines.

In terms of where this study may go in the future, extrapolating beyond the data points measured for this variable temperature analysis and assuming that the contraction along a and b continues to be linear, it is not hard to envisage that there may come a point where the van der Waals forces in these directions become optimised and the only way left for the molecule to move is about the C1–C1' bond. In this scenario, due to the alignment of the the BINOL molecule with respect to the [001] direction, the molecule should start to spread out in the (001) plane, extending the a and b axes and hence the crystal may exhibit negative thermal expansion (NTE).

Supplementary Information The online version contains supplementary material available at <https://doi.org/10.1007/s10870-024-01013-6>.

Acknowledgements The author thanks the Engineering and Physical Sciences Research Council for the X-ray crystallography instrumentation used in this study (EP/F03637X/1). Thanks also to Dr Lee J. Higham for supplying the (R)-BINOL and Dr Oleg V. Dolomanov for helpful discussions regarding molecular geometry.

Author Contributions All of the experimental work, analysis and manuscript preparation were performed by PGW.

Data Availability CCDC 2333325–2,333,329 contain the full crystallographic data for this article. These are available free of charge at www.ccdc.cam.ac.uk/data_request/cif, by emailing data_request@ccdc.cam.ac.uk or by contacting The Cambridge Crystallographic Data Centre, 12 Union Road, Cambridge, CB2 1EZ, UK, fax: +44 1223 336033.

Declarations

Competing interests The author declares no competing financial interests.

Open Access This article is licensed under a Creative Commons Attribution 4.0 International License, which permits use, sharing, adaptation, distribution and reproduction in any medium or format, as long as you give appropriate credit to the original author(s) and the source, provide a link to the Creative Commons licence, and indicate if changes were made. The images or other third party material in this article are included in the article's Creative Commons licence, unless indicated otherwise in a credit line to the material. If material is not included in the article's Creative Commons licence and your intended use is not permitted by statutory regulation or exceeds the permitted use, you will need to obtain permission directly from the copyright holder. To view a copy of this licence, visit <http://creativecommons.org/licenses/by/4.0/>.

References

- Krishnan RS, Srinivasan R, Devanarayanan S (1979) Thermal expansion of crystals. Pergamon Press, Oxford
- Kim HJ, Lee E, Park HS, Lee M (2007) Dynamic extension-contraction motion in supramolecular springs. *J Am Chem Soc* 129:10994
- Tanaka K, Osuga H, Kitahara Y (2000) Clathrate formation by and self-assembled supramolecular structures of a “molecular spring.” *J Chem Soc Perkin Trans 2*:2492
- Zięba S, Rusek M, Katrusiak A, Gzella A, Dubis AT, Łapiński A (2023) Helical model of compression and thermal expansion. *Sci Rep* 13:17398
- Perrot A, Moulin E, Giuseppone N (2021) Extraction of mechanical work from stimuli-responsive molecular systems and materials. *Trends Chem* 3:926
- Jin M, Kitsu R, Hammyo N, Sato-Tomita A, Mizuno M, Mikherdov AS, Tsitsvero M, Lyalin A, Taketsugu T, Ito H (2023) A steric-repulsion-driven clutch stack of triaryltriazines: correlated molecular rotations and a thermoresponsive gearshift in the crystalline solid. *J Am Chem Soc* 145:27512
- Mei L, An SW, Hu KQ, Wang L, Yu JP, Huang ZW, Kong XH, Xia CQ, Chai ZF, Shi WQ (2020) Metal-organic materials molecular spring-like triple-helix coordination polymers as dual-stress and thermally responsive crystalline metal-organic materials. *Angew Chem Int Ed* 59:16061
- Juneja N, Unruh DK, Hutchins KM (2023) Engineering colossal anisotropic thermal expansion into organic materials through dimensionality control. *Chem Mater* 35:7292
- Mori K, Masuda Y, Kashino S (1993) (+)-(R)- and racemic forms of 2,2'-dihydroxy-1,1'-binaphthyl. *Acta Cryst C* 49:1224
- Toda F, Tanaka K, Miyamoto H, Koshima H, Miyahara I, Hirotsu K (1997) Formation of racemic compound crystals by mixing of two enantiomeric crystals in the solid state: liquid transport of molecules from crystal to crystal. *J Chem Soc Perkin Trans 2*:1877
- Lee T, Peng JF (2010) Photoluminescence and crystal structures of chiro-optical 1,1'-Bi-2-naphthol crystals and their inclusion compounds with dimethyl sulfoxide. *Cryst Growth Des* 10:3547
- Zhang X, Chen L, Chen XY, Zhang H, Yang L, Yang F (2016) Effective separation of single-walled carbon nanotubes and their very different electrochemical behaviours. *Chem Commun* 52:9287
- Tyler AR, Ragbirsingh R, McMonagle CJ, Waddell PG, Heaps SE, Steed JW, Thaw P, Hall MJ, Probert MR (2020) Encapsulated nanodroplet crystallization of organic-soluble small molecules. *Chem* 6:1755
- Ye Y, Cook TR, Shu-Ping Wang SP, Wu J, Li S, Stang PJ (2015) Self-assembly of chiral metallacycles and metallacages from a directionally adaptable BINOL-derived donor. *J Am Chem Soc* 137:11896
- CrysAlisPro. Rigaku Oxford Diffraction, Tokyo, Japan
- Sheldrick GM (2015) Crystal structure refinement with SHELXL. *Acta Crystallogr Sect A Found Crystallogr* 71:3
- Sheldrick GM (2008) A short history of SHELX. *Acta Crystallogr Sect A Found Crystallogr* 64:112
- Dolomanov OV, Bourhis LJ, Gildea RJ, Howard JAK, Puschmann H (2009) OLEX2: a complete structure solution, refinement and analysis program. *J Appl Cryst* 42:339
- Cliffe MJ, Goodwin AL (2012) PASCAL: a principal axis strain calculator for thermal expansion and compressibility determination. *J Appl Cryst* 45:1321
- Etter MC (1990) Encoding and decoding hydrogen-bond patterns of organic compounds. *Acc Chem Res* 23:121
- Spackman PR, Turner MJ, McKinnon JJ, Wolff SK, Grimwood DJ, Jayatilaka D, Spackman MA (2021) *CrystalExplorer*: a program for Hirshfeld surface analysis, visualization and quantitative analysis of molecular crystals. *J Appl Cryst* 54:1006
- Desiraju GR, Steiner T (1999) *The weak hydrogen bond. Structural chemistry and biology*. Oxford University Press, Oxford
- Wood PA, Allen FH, Pidcock E (2009) Hydrogen-bond directionality at the donor H atom—analysis of interaction energies and database statistics. *CrystEngComm* 11:1563

Publisher's Note Springer Nature remains neutral with regard to jurisdictional claims in published maps and institutional affiliations.